Inorganica Chimica Acta, 141 (1988) 193–199

Structural and Magnetic Properties of Bis(ethanolammonium)hexahalodicuprate(II) Salts: Copper(II) Halide Dimers with a Square-pyramidal Type Distortion

BRIAN SCOTT and ROGER WILLETT

Chemical Physics Program, Washington State University, Pullman, Wash. 99164, U.S.A.

(Received April 2, 1987)

Abstract

The compounds $(C_4H_{16}N_2O_2)Cu_2Cl_6$ and $(C_4H_{16}N_2O_2)Cu_2Br_6$ have been synthesized and their crystal structures determined. EPR and magnetic susceptibility measurements were made. The crystals of both compounds are triclinic, space group $P\bar{1}$ with a = 6.077(1), b = 8.068(2), c = 8.455(2) Å, α = 67.99(2), β = 79.90(2), γ = 78.77(2)°, Z = 2, and D_{calc} = 2.08 g/cm^3 for the chloride salt, and a = 6.418(2), b = 8.262(2), c = 8.764(2) Å, α = 68.17(2), β = 80.12(2), γ = 78.47(2)°, Z = 2, and D_{calc} = 2.88 for the bromide salt. The structures, solved by direct methods and refined by least-squares calculations to R = 0.036 (chloride) and R = 0.049 (bromide), consist of nearly planar $Cu_2X_6^{2-}$ dimers stacked to form infinite chains. The coordination of the copper atoms may be described as distorted square pyramidal with an ethanolammonium oxygen semi-coordinated to the sixth coordination site for each copper atom. Both compounds exhibit predominantly antiferromagnetic exchange interactions. The bromide salt exhibits a intradimer singlet–triplet energy splitting of $J/k = -64$ K and a interdimer splitting of $J'/k = -21$ K, while for the chloride $J/k = -6$ K and $J'/k = -6$ K is deduced. A comparison with the magnetic behavior of other $Cu_2X_6^{2-}$ dimers is given.

Introduction

In recent years the magnetostructural properties of several copper(II) halide dimers have been studied [1, 2]. In all cases these dimers have been found to be either planar, bifolded or twisted [3]. For the planar dimers antiferromagnetic behavior is increased with increasing bridging angle, ϕ. The bifold distortion is characterized by the bifold angle, σ, between the central Cu_2X_2 plane and the terminal CuX_3 planes. The twist distortion is characterized by a twist angle, τ, between the bridging Cu_2X_2 plane and the terminal CuX_2 planes (Fig. 1). These studies have shown that for the chloride salts with a bifold distortion (with $\phi \approx 95.5$), J is antiferromagnet

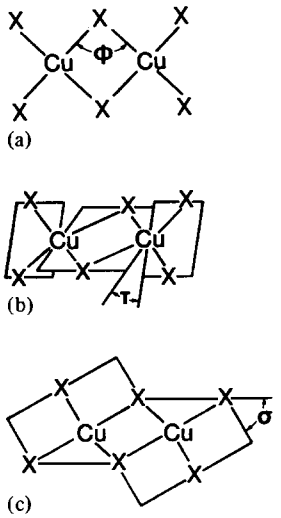

Fig. 1. Distortion of the $Cu_2X_6^{2-}$ dimeric species; (a) planar; (b) twisted; (c) bifolded.

for small values of σ and becomes ferromagnetic for $\sigma \geqslant 25$ [4]. It has also been observed that the exchange coupling is antiferromagnetic for $\tau = 0$, becomes ferromagnetic for $\tau = 50$, and becomes antiferromagnetic again for $\tau \approx 85$ [5, 6]. In this paper magnetic susceptibility measurements for two new copper(II) halide dimers are reported; (ethanolammonium)$_2Cu_2Cl_6$ and (ethanolammonium)$_2Cu_2Br_6$.

Experimental

Bis(ethanolammonium)hexachlorodicuprate(II), $(EOA)_2Cu_2Cl_6$, was prepared by dissolving stoichiometric amounts of ethanolamine and cupric chloride in a moderately dilute aqueous HCl solution and crystallizing by slow evaporation at room temperature. The corresponding bromide, $(EOA)_2Cu_2Br_6$, was prepared in a similar manner. The crystals grow as dark red (Cl) or opaque purple (Br) needles.

The crystal structures of these triclinic salts were determined at room temperature. The data collection was carried out on a Nicolet R3m/E system

0020-1693/88/$3.50

TABLE I. X-ray Data Collection Parameters

Compound name	ethanolammonium trichlorocuprate(II)	ethanolammonium tribromocuprate(II)
Empirical formula	$C_4H_{16}N_2O_2Cu_2Cl_6$	$C_4H_{16}N_2O_2Cu_2Br_6$
Molecular weight	464	731
Diffractometer system	Nicolet R3m/E	Nicolet R3m/E
Crystal class	triclinic	triclinic
Space group	$P\bar{1}$	$P\bar{1}$
Systematic absence	none	none
Lattice contants		
a (Å)	6.077(1)	6.418(2)
b (Å)	8.068(2)	8.262(2)
c (Å)	8.455(2)	8.764(2)
α (°)	67.99(2)	68.17(2)
β (°)	79.20(2)	80.12(2)
γ (°)	78.77(2)	78.47(2)
V (Å^3)	374.4(2)	420.2(2)
	based on 25 reflections in the range $30 < 2\theta < 33$	based on 25 reflections in the range $24 < 2\theta < 29$
$F(000)$	232	338
Radiation	Mo Kα with graphite monochromator	Mo Kα with graphite monochromator
Crystal size	0.3 X 0.5 X 0.6 mm	0.33 X 0.17 X 0.13 mm
Absorption coefficient	39.4	83.32
Calculated density	$\rho = 2.08$ ($Z = 2$)	$\rho = 2.88$ ($Z = 2$)
Type of absorption correction	empirical (ellipsoidal)	empirical (ellipsoidal)
maximum transmission	0.86	0.024
minimum transmission	0.52	0.006
Data collection technique	ω scan	ω scan
Scan range	2°	2°
Scan speed	6°/min (min)	2.00°/min (min)
	29.3°/min (max)	29.3°/min (max)
Check reflections	1 0 1, 1 0 −1, 1 2 −1	−2 2 1, −3 0 3
monitored every 100 reflections		
Total reflections	2350	2108
2θ (max)	50	55
unique reflections	2158 with 1984 with $F > 3\sigma(F)$	1930 with 1466 with $F > 3\sigma(F)$
R for equivalent reflections	0.021	0.0274
Structure solution package	Nicolet SHELXTL	Nicolet SHELXTL
Structure solution technique	direct methods	Patterson
$R = \Sigma\|\|F_o\| - \|F_c\|\|/\|F_o\|$	0.036	0.0492
$R_w = \text{SQRT}[\Sigma w(\|F_o\| - \|F_c\|)^2/\Sigma w\|F_o\|^2]$:	0.0397	0.0472
with $w = 1/[\sigma^2(F) + g(F)^2]$	$g = 0.00125$	$g = 0.00028$
$\|\Delta/\sigma\|$ (mean)	0.003	0.001
$\|\Delta/\sigma$ (max)	0.045	0.004
Total parameters refined	75	74
thermal parameters	anisotropic on all non-hydrogen atoms	anisotropic on all non-hydrogen atoms
hydrogen atoms	constrained to C–H and N–H = 0.96 Å, thermal parameters fixed at 0.10	constrained to C–H and N–H = 0.96 Å, thermal parameters fixed at 0.10
Largest peak on final difference map	1 e$^-$/Å^3 near: Cu	1 e$^-$/Å^3 near: Cu
Extinction corrections	0.01183	0.00887
Goodness of fit	1.19	1.285

[7]. The orientation matrix and lattice parameters of the triclinic crystals were optimized from the least-squares refinement to the angular settings of 25 carefully centered reflections with high Bragg angles. Details of the data collection are given in Table I. Mo Kα radiation ($\lambda = 0.71069$ Å) was used, with a graphite monochromator. The SHELXTL 4.1 software package was used for data reduction and refinement [8].

Magnetic measurements on the two compounds in the liquid nitrogen range (80–300 K) were taken at Washington State University on a PAR vibrating-sample magnetometer. Liquid helium range data (5–80 K) were taken at Clark University on a PAR vibrating sample magnetometer.

EPR powder measurements were taken with a Varian E-3 spectrometer at both room and liquid nitrogen temperatures.

TABLE II. Atomic Coordinates ($\times 10^4$) and Isotropic Thermal Parameters ($Å^2 \times 10^3$) for $(EOA)_2Cu_2Br_6$ and $(EOA)_2Cu_2Cl_6$

	x	*y*	*z*	*U*[a]
$(EOA)_2Cu_2Br_6$				
Br(2)	−761(1)	2455(1)	4363(1)	47(1)*
Br(1)	3763(1)	882(1)	6380(1)	44(1)*
Br(3)	2203(2)	1204(2)	1082(1)	51(1)*
Cu	2625(2)	716(2)	3905(1)	43(1)*
N	2785(13)	7465(11)	59(9)	52(3)*
O	5182(15)	4313(12)	2131(10)	84(4)*
C(1)	1949(17)	6274(14)	1734(12)	55(4)*
C(2)	3676(19)	5447(14)	2814(12)	58(4)*
$(EOA)_2Cu_2Cl_6$				
Cu	2663(1)	728(1)	3898(1)	22(1)*
Cl(1)	3757(1)	828(1)	6358(1)	24(1)*
Cl(2)	−731(1)	2356(1)	4341(1)	26(1)*
Cl(3)	2245(1)	1140(1)	1161(1)	30(1)*
N	2691(4)	7531(3)	90(3)	31(1)*
C(1)	1770(5)	6337(4)	1799(4)	32(1)*
C(2)	3600(5)	5412(4)	2951(4)	34(1)*
O	5055(4)	4184(4)	2263(3)	51(1)*

[a]Starred items: the equivalent isotropic *U* is defined as one-third of the trace of the orthogonalized U_{ij} tensor.

Results

Chloride Structure

The coordinates of the copper and chloride atoms were found from direct methods. The positions of the carbon, nitrogen and oxygen atoms were located from subsequent difference Fourier maps. Several cycles of least-squares refinement of positional and isotropic thermal parameters were performed. Final refinement included variation of all positional parameters and anisotropic thermal parameters on the Cu, Cl, C, and O atoms. Protons were refined with rigid-body constraints and isotropic thermal parameters fixed at approximately 1.2 times the corresponding heavy-atom thermal parameter. Final values of R = 0.036 and R_w = 0.040 were obtained for all reflections with $F \geqslant 3\sigma$ and $2\theta \leqslant 50°$.

Bromide Structure

Analysis of the Patterson function generated positional parameters for the Cu and Br atoms. The C, N and O atoms were located from subsequent difference Fourier maps and the protons were treated as in the chloride structure above. Final values of $R = 0.049$ and $R_w = 0.050$ were obtained with $F \geqslant 3\sigma$ and $2\theta \leqslant 55°$. Final positional parameters and equivalent isotropic thermal parameters are given in Table II.

Structure Descriptions

The structures of the chloride and bromide salts have dimers which form chains of stacking dimers, as shown in Fig. 2 for the bromide salt. Interatomic distances and angles are given in Table III for the two compounds. The coordination geometry around each copper(II) ion consists of four short Cu–X bonds, one longer semi-coordinate Cu–X bond, and a longer semi-coordinate Cu–O bond. This geometry can be characterized as being intermediate between a square-pyramidal and a 4 + 2 elongated octahedral geometry. Within the basal plane, the *trans* X–Cu–X angles are 171.1(1)° and 165.2(1)° (Cl) and 173.2(1)° and 163.0(1)° (Br). These compounds do not undergo a true bifold distortion due to their square-pyramidal type geometry and this must be taken in account when looking at the bifold angles. If the geometrical distortion is approximated as a bifold type, angles of 13.8° (Cl) and 14.9° (Br) are calculated, assuming X(3) is the halide ion distorted out of the plane. The bridging angles and bond lengths

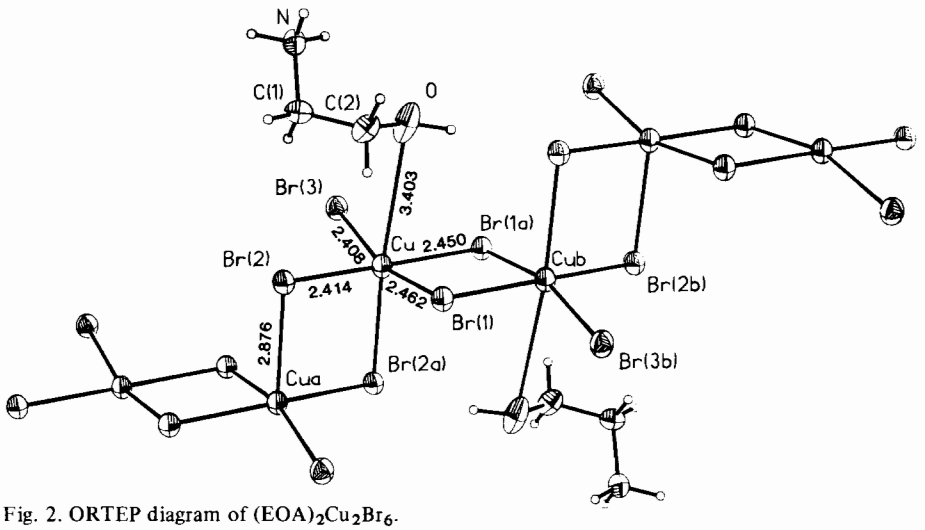

Fig. 2. ORTEP diagram of $(EOA)_2Cu_2Br_6$.

TABLE III. Bond Lengths (Å) and Angles (°) for $(EOA)_2Cu_2X_6$[a]

	Br	Cl
Bonds		
Cu–X(1)	2.462(2)	2.321(1)
Cu–X(2)	2.414(1)	2.267(1)
Cu–X(3)	2.408(2)	2.259(1)
Cu–X(1a)	2.450(1)	2.304(1)
Cu–X(2a)	2.876(2)	2.739(1)
Cu–O	3.403(8)	3.128(3)
O–C(2)	1.424(15)	1.416(4)
C(2)–C(1)	1.472(15)	1.498(4)
C(1)–N	1.509(11)	1.484(3)
Angles		
X(1)–Cu–X(2)	89.5(1)	90.2(1)
X(1)–Cu–X(3)	163.0(1)	165.2(1)
X(2)–Cu–X(3)	94.3(1)	94.2(1)
X(2)–Cu–X(1a)	173.2(1)	174.1(1)
X(1)–Cu–X(2a)	95.2(1)	93.4(1)
X(3)–Cu–X(2a)	101.4(1)	100.9(1)
Cu–X(2)–Cu(a)	90.1(1)	91.7(1)
X(1)–Cu–X(3)	163.0(1)	165.2(1)
X(1)–Cu–X(1a)	84.3(1)	84.1(1)
X(3)–Cu–X(1a)	90.8(1)	90.9(1)
X(2)–Cu–X(2a)	89.9(1)	88.3(1)
Cu–X(1)–Cu(b)	95.7(1)	95.9(1)
N–C(1)–C(2)	110.9(8)	111.2(2)
C(1)–C(2)–O	108.7(10)	107.8(3)
Cu–O–C(2)	96.5(5)	102.1(2)

[a]The symmetry related atoms are denoted with a and b (Fig. 2).

for the chloride and bromide salts are 95.9(1)°/2.321(1) Å and 95.7(1)°/2.462(2) Å respectively.

Magnetics

The magnetic susceptibility of the bromide salt reaches a maximum at 75 K (Fig. 3), while for the chloride salt, a maximum is reached near 8 K (Fig. 4). The structural data would indicate that it is appropriate to interpret the results in terms of an alternating chain model. The Hamiltonian for an alternating chain may be written as

$$\mathcal{H} = -2J\sum_{i=1}^{N/2}(S_{2i-1}S_{2i} + \alpha S_{2i}S_{2i+1})$$

The temperature at the maximum uniquely defines the strongest antiferromagnetic coupling within the chain since the susceptibility of the alternating antiferromagnetic chain reaches a maximum at $T_{max} \cong 1.25\ (J/k)$. This fixes $J/k \cong -60$ K and -6 K for the bromide and chloride salts respectively. A least-squares fit to the alternating-chain model [6] yields $J/k = -61.4(2)$ and $J'/k = -21.3(2)$, where $J' = \alpha J$, with $g = 2.08$ and 4.0(2) percent impurity for the bromide salt. The chloride salt was fit to the same model yielded $J/k = -6.0(3)$ and $J'/k = -5.9(3)$ with $g = 2.05$ and 7.9(2) percent impurity. Since exchange coupling associated with asymmetrical bridges is known to be invariably weak it may be assumed that the larger J value for the bromide salt corresponds to intradimer exchange and the smaller J value corresponds to interdimer coupling. In the chloride salt J and J' are approximately the same, which indicates that the interdimer and intradimer coupling are nearly equivalent, and that the system behaves essentially as a linear chain.

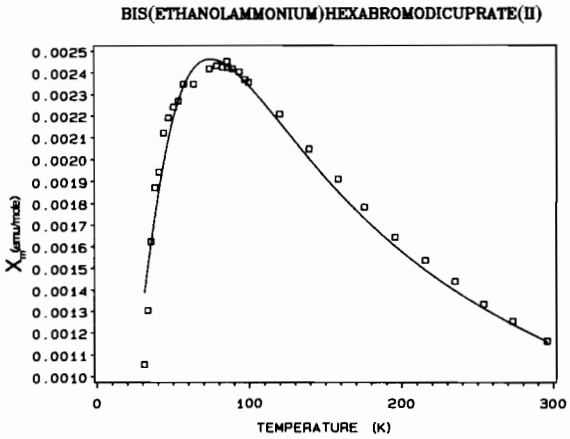

Fig. 3. Plot of χ_M *vs.* T for $(EOA)_2Cu_2Br_6$.

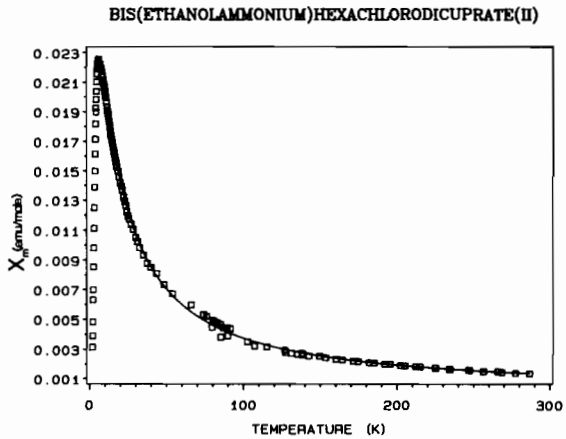

Fig. 4. Plot of χ_M *vs.* T for $(EOA)_2Cu_2Cl_6$.

EPR

The EPR spectrum of $(EOA)_2Cu_2Cl_6$ at room temperature consists of a single broad line ($\Delta H \cong$ 450 Oe) containing obvious, but unresolved structure. At liquid nitrogen, the linewidth has decreased sufficiently that an axial powder spectrum is revealed with $g_\parallel \approx 2.21$ and $g_\perp \approx 2.07$ with a linewidth of roughly 150 Oe. The g values are in the range associated with 4 + 2 coordinate copper halides and

in the absence of single crystal data, the $g_\parallel$ axis can reasonably be assumed to be perpendicular to the plane of the $Cu_2Cl_6^{2-}$ dimer. No half field line is observed, consistent with the linear chain nature of the exchange-coupled system. The EPR linewidths of exchange-coupled copper(II) halide salts are known to exhibit a linear temperature dependence [10, 11], so the broader linewidth at room temperature is not surprising.

In contrast to the relatively simple and expected EPR spectra for the chloride salt, $(EOA)_2Cu_2Br_6$ shows a much different behaviour. At room temperature, a single, extremely broad line is observed, with linewidth in excess of 5000 Oe. At 78 K, this line has narrowed somewhat ($\Delta H \approx 3500$ Oe). In addition, a much narrower powder spectrum now appears with $\Delta H \approx 40$ Oe. However, this is an inverted spectrum, with $g_\perp \approx 2.26$ and $g_\parallel \approx 2.05$, of the type normally associated with a coordination geometry closer to trigonal bipyramidal [12]. The broader line is interpreted as arising from the $(Cu_2Br_6^{2-})_n$ chains. It is known that the EPR linewidths of copper(II) bromide salts are substantially larger than the corresponding chlorides (by more than an order of magnitude) due to the larger ligand spin–orbit coupling [13]. In addition, the linewidths increase roughly as J^4. Thus, the observation of extremely large EPR lines for this exchange coupled system is not surprising. The source of the inverted EPR spectrum at 78 K is more puzzling. It is consistent, however, with EPR spectra on a wide series of stacked $Cu_2X_6^{2-}$ dimers [14]. Tentatively, it is assumed that these spectra arise from intrinsic impurities arising from lattice defects. A detailed description of the nature of these impurities awaits single crystal EPR studies. A reasonable postulate to consider involves the loss of a CuX_2 group from one of the dimers in the chain. This would allow the remaining CuX_4^{2-} moiety, with its semi-coordinate bond to an adjacent dimer, to distort towards a trigonal bipyramidal geometry. It would also create a break in the dimer chain, leaving an odd number of spins present. This would account for the so-called paramagnetic 'tail' seen at low temperatures in most antiferromagnetic dimer chains. An unresolved question at this time involves the issue of why this impurity spin is uncoupled from the spins in the chain and why it appears as an independent spectrum.

Discussion

One of the goals of magneto-structural studies is to obtain correlations between structural and/or electronic properties of a system and their corresponding magnetic behavior. The results obtained here are relevant to two such relationships which we have been investigating in our laboratory: the role of the ligand-to-metal charge-transfer energies upon the exchange coupling and the effect of distortion of the $Cu_2X_6^{2-}$ ion from planarity.

Figure 5 shows a plot of magnetic exchange constants for copper(II) chloride *versus* bromide salts. It is seen that for most of the ferromagnetic

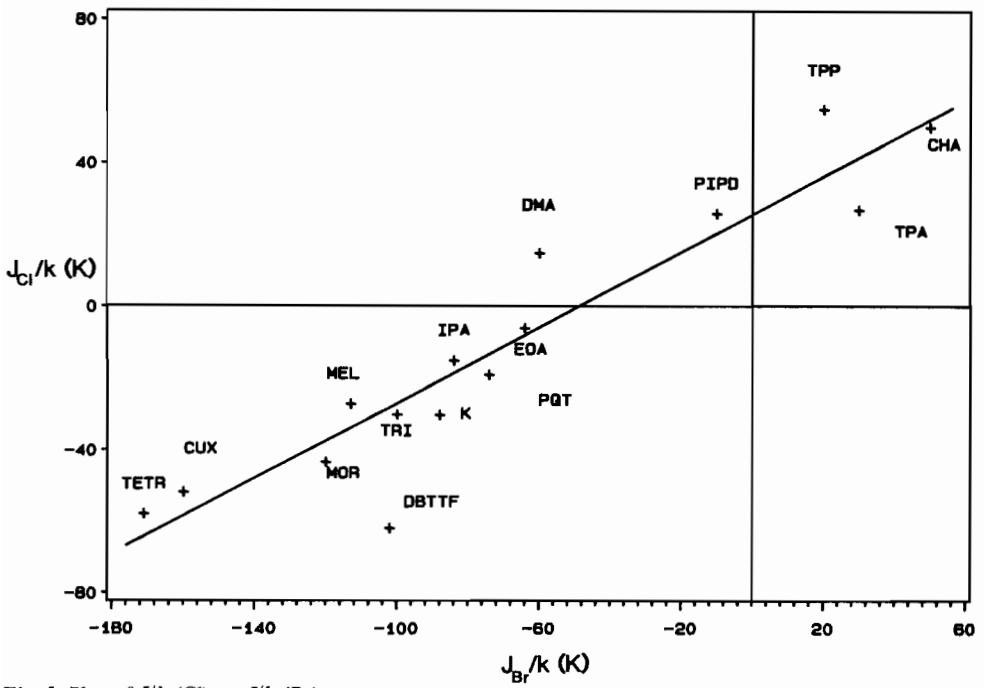

Fig. 5. Plot of J/k (Cl) *vs.* J/k (Br).

salts in the series, the magnitude of J/k is approximately the same irrespective of the ligand. This trend changes as the salts become more antiferromagnetic; J/k decreases much more rapidly for the bromide salts than for the chloride salts. These differences may not be explained by structural arguments since little change in structure occurs between the chloride and bromide salts, as seen in this study. However, if the factors influencing the antiferromagnetic exchange to coupling are examined, an explanation is discovered [15]. In the Hoffmann [16] formalism, the exchange is expressed as

$$2J = 2J_F - (\epsilon_s - \epsilon_a)^2/(J_{aa} - J_{bb})$$

Here J_{aa} and J_{ab} are one- and two-center Coulomb integrals, while ϵ_s and ϵ_a are the one-electron energies of the symmetric and antisymmetric combination of magnetic orbitals on the two metal centers. It may be seen from this equation that the antiferromagnetic contribution goes as $(\epsilon_s - \epsilon_a)^2$, and that the interaction becomes more ferromagnetic as ϵ_a approaches ϵ_s. Hay *et al.* argue that this antiferromagnetic term is inversely proportional to the difference in energies between the ligand orbitals and the magnetic orbital on the metal. This quantity may be estimated from the intense ligand-to-metal charge-transfer transitions, which occur at the UV–Vis borderline for the chloride salts (25 000–30 000 cm^{-1}) but are in the middle of the visible region for the bromide salts (15 000–20 000 cm^{-1}). It may be postulated from these data that the antiferromagnetic contribution to the exchange, J_{AF}, will be 2–3 times larger for the bromide than for the chloride salts. This is in excellent agreement with the experimental trends, as can be seen in Fig. 5. A rough linear relationship is readily observed, with a slope of approximately 1/2.

In Fig. 6, a plot of J/k *versus* the bifold angle, σ, is given for the series of $Cu_2X_6^{2-}$ dimers studied to date. In general, a relatively smooth correlation is observed. Table IV summarizes the magnetic and structural data for these compounds. Included are the calculated $\epsilon_s - \epsilon_a$ values for the chloride salts. These data show that the exchange coupling becomes more antiferromagnetic with increasing bridging angle, and more ferromagnetic with increasing bifold angle. Also, the calculated values of $\epsilon_s - \epsilon_a$ closely correlate with these trends, indicating that it is the antiferromagnetic nature of the coupling which is changing during the geometrical distortion. As can be seen from Fig. 6, if the J/k values for the EOA salts are plotted against the nominal bifold value described in 'Structure Description', it lies substantially off of the predicted curve. However, the distortion is more of a square-pyramidal nature, and so all terminal halides are displaced off the bridging Cu_2X_2 plane. Qualitatively, then, the data can be understood if J/k is correlated with the sum of the two possible bifold angles which would be approximately 20°. Unfortunately, the calculated $\epsilon_s - \epsilon_a$ values, for the chloride salt, based on the actual geometry, do not back this.

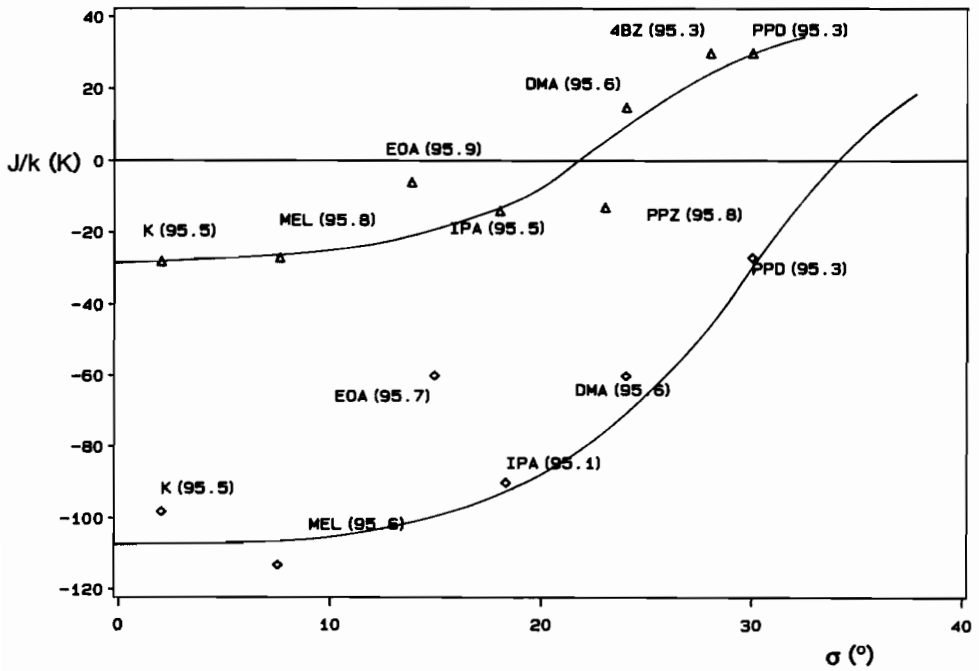

Fig. 6. Plot of J/k *vs.* σ for $Cu_2X_6^{2-}$ dimers.

TABLE IV. Structural and Magnetic Parameters of Stacked Planar or Sedia $Cu_2X_6^{2-}$ Dimers[a]

Cation	X = Cl					X = Br			
	ϕ (°)	Cu–Cl, bridging (Å)	σ (°)	J/k (K)	$\epsilon_s - \epsilon_a$ (eV)	ϕ (°)	Cu–Br, bridging (Å)	σ (°)	J/k (K)
K^+	95.5	2.318	1.5	−28	0.1153				−95
2-amino-3-hydroxy-pyridinium$^+$						97.0	~2.460	~6.3	
$CH_2OHCH_2NH_3^+$ [b]	95.9	2.312	13.8	−6	0.1182	95.7	2.456	14.9	−60
Melaminium^{2+}	95.8	2.334	7.6	−28	0.1140	95.6	2.468	7.5	−113
$Me_4enH_2^{2+}$	96.4	2.322	17.9	−23	0.1130	95.7	2.451	17.1	−134
$(CH_3)_2CHNH_3^+$	95.5	2.308	19.2	−14	0.1125	95.1	2.446	18.3	−90
Piperazinium^{2+}	95.8	2.324	23.2	−13	0.1093				
$(CH_3)_2NH_2^+$	95.6	2.326	23.6	~15	0.1018				−60
Piperidinium$^+$	95.5	2.288	29.6	26	0.1042				−9
4-$\phi CH_2C_5H_{11}N^+$	95.3	2.311	28.7	30	0.0916				
$MeNH_2C_2H_4\phi^+$	95.1	2.339	46.1	70					
Paraquat^{2+}	97.5	2.318	31.7	−19	0.111				−74

[a]Refs. 16 and 17 and refs. therein. [b]The distortion in this salt yields a geometry closer to square-pyramidal.

Conclusion

This study confirms that the magnetic properties of copper(II) halide salts are influenced greatly by the chemistry of the halide ion. The existence of lower lying charge-transfer states in the bromide salts enhances the antiferromagnetic contribution to the exchange as compared to the chloride salts. Thus, despite their similar structural characteristics, the magnetic behavior of copper(II) chloride and bromide salts are greatly modified by variations in the electronic structure of the halide ions. In addition, the anomalous behavior for the ethanolammonium salts supports the idea that the square-pyramidal type distortion is important when considering magneto-structural correlations.

Supplementary Material

Listings of anisotropic thermal parameters and H atom coordinates and isotropic thermal parameters; listings of observed and calculated structure factors are available from the authors on request.

Acknowledgements

This work was supported by NSF Grant DMR 8219430. The Nicolet R3m/E facility was established through funds provided by NSF grant CHE 8408407 and by Boeing Company. The use of the facilities of Prof. C. P. Landee of Clark University in collecting the low temperature susceptibiliy is appreciated, as is the assistance of Mr Baldev Patayl in collection and analysis of the EPR data.

References

1 R. D. Willett, in R. D. Willett, D. Gatteschi and O. Kahn (eds.), 'Magneto-Structural Correlations in Exchange Coupled Systems', NATO ASI Series, Plenum, New York, 1985, p. 389.
2 W. H. Hatfield, in R. D. Willett, D. Gatteschi and O. Kahn (eds.), 'Magneto-Structural Correlations in Exchange Coupled Systems', NATO ASI Series, Plenum, New York, 1985, p. 555.
3 R. D. Willett and U. Geiser, *Acta Chem. Croat., 57*, 751 (1984).
4 L. P. Battaglia, A. Bonamartini-Corradi, U. Geiser, R. D. Willett, A. Motori, F. Sandrolini, L. Antolini, T. Manfredini, L. Menabue and G. C. Pellacani, *J. Chem. Soc., Dalton Trans.*, 1987, in press.
5 A. Bencini, D. Gatteschi and C. Zanchini, *Inorg. Chem., 24*, 700 (1985).
6 R. Fletcher, S. O'Brien, D. R. Bloomquist, J. J. Hansen and R. D. Willett, *Inorg. Chem., 22*, 330 (1983).
7 C. F. Campana, D. F. Shepard and W. M. Litchman, *Inorg. Chem., 20*, 4039 (1981).
8 G. Sheldrick, 'SHELXTL', Nicolet Analytical Instruments, Madison, Wis., 1984.
9 J. W. Hall, W. E. Marsh, R. R. Weller and W. E. Hatfield, *Inorg. Chem., 20*, 1033 (1981).
10 R. D. Willett, R. J. Wong and M. Numata, *Inorg. Chem., 22*, 3189 (1983).
11 T. M. Kite, J. E. Drumheller and K. Emerson, *J. Magn. Reson., 48*, 20 (1982).
12 B. J. Hathaway, *Coord. Chem. Rev., 41*, 425 (1982).
13 R. J. Wong and R. D. Willett, *J. Magn. Reson., 42*, 446 (1981).
14 Baldev Patyal, private communication.
15 R. D. Willett, *Inorg. Chem., 25*, 1918 (1986), and refs. therein.
16 P. J. Hay, J. C. Blanchard and R. J. Hoffmann, *J. Am. Chem. Soc., 97*, 4884 (1975).
17 R. D. Willett, T. Grigereit, K. Halvorson and B. Scott, *Proc. Ind. Acad. Sci., 98*, 147 (1987).